NASA TECHNICAL MEMORANDUM

NASA TM X-71943

COPY NO.

NASA TM X- 71943

THE EFFECTS OF SHOT-PEENING RESIDUAL STRESSES ON THE FRACTURE AND CRACK GROWTH PROPERTIES OF D6AC STEEL

by Wolf Elber

NASA Langley Research Center
Hampton, VA 23665

Presented at the ASTM Seventh National Symposium
on Fracture Mechanics, College Park, MD,
August 27-29, 1973

NATIONAL AERONAUTICS AND SPACE ADMINISTRATION
LANGLEY RESEARCH CENTER, HAMPTON, VIRGINIA 23665

1. Report No.	2. Government Accession No.	3. Recipient's Catalog No.
TM X-71943		

4. Title and Subtitle	5. Report Date
The Effects of Shot-Peening Residual Stresses on the Fracture and Crack-Growth Properties of D6AC Steel	6. Performing Organization Code
7. Author(s)	8. Performing Organization Report No.
Wolf Elber	10. Work Unit No.
9. Performing Organization Name and Address	11. Contract or Grant No.
NASA Langley Research Center Hampton, VA 23665	13. Type of Report and Period Covered
12. Sponsoring Agency Name and Address	14. Sponsoring Agency Code
National Aeronautics and Space Administration Washington, DC 20546	

15. Supplementary Notes

16. Abstract

The fracture strength and cyclic crack-growth properties of surface-flawed, shot-peened D6AC steel plate were investigated. For short crack lengths (up to 1.5mm) simple linear elastic fracture mechanics - based only on applied loading - did not predict the fracture strengths. Also, Paris' Law for cyclic crack growth did not correlate the crack-growth behavior. To investigate the effect of shot-peening, additional fracture and crack-growth tests were performed on material which was precompressed to remove the residual stresses left by the shot-peening. Both tests and analysis show that the shot-peening residual stresses influence the fracture and crack-growth properties of the material. This report presents the analytical method of compensating for residual stresses and the fracture and cyclic crack-growth test results and predictions.

17. Key Words (Suggested by Author(s)) (STAR category underlined)	18. Distribution Statement
Materials, Metallic, Structural Mechanics, fracture, crack-growth, residual stresses	

19. Security Classif. (of this report)	20. Security Classif. (of this page)	21. No. of Pages	22. Price*
Unclassified	Unclassified	21	$3.00

*Available from { The National Technical Information Service, Springfield, Virginia 22151
STIF/NASA Scientific and Technical Information Facility, P.O. Box 33, College Park, MD 20740

THE EFFECTS OF SHOT-PEENING RESIDUAL STRESSES ON THE FRACTURE AND CRACK-GROWTH PROPERTIES OF D6AC STEEL

Wolf Elber

NASA Langley Research Center

Hampton, Virginia

Summary

The fracture strength and cyclic crack-growth properties of surface-flawed, shot-peened D6AC steel plate were investigated. For short crack lengths (up to 1.5 mm) simple linear elastic fracture mechanics – based only on applied loading – did not predict the fracture strengths. Also, Paris' Law for cyclic crack growth did not correlate the crack-growth behavior. To investigate the effect of shot-peening, additional fracture and crack-growth tests were performed on material which was precompressed to remove the residual stresses left by the shot-peening. Both tests and analysis show that the shot-peening residual stresses influence the fracture and crack-growth properties of the material. This report presents the analytical method of compensating for residual stresses and the fracture and cyclic crack-growth test results and predictions.

Introduction

When a material is shot-peened, the residual compressive stresses at the surface prolong the fatigue life. A recent investigation of the fracture and cyclic crack-growth properties of shot-peened surface-flawed D6AC steel revealed some anomalies in these properties. The present study was conducted to show that the residual stresses at the surface caused these anomalies. The study was both experimental and analytical.

A simple mathematical model was constructed to evaluate the contribution of the residual stresses to the stress intensity. For an assumed residual

stress distribution, the effect of the residual stresses explained the discrepancies between the experimental results and the linear elastic fracture mechanics analysis. In a series of tests, specimens were precompressed to a permanent compressive strain of 0.1 percent to remove the residual stresses left by shot-peening. Fracture and cyclic crack-growth tests showed that the properties were in good agreement with linear elastic fracture mechanics analysis.

List of Symbols

A,B	Compliance gage calibration constants
a	Depth of surface crack (m)
b	Distance of concentrated force from free surface (m)
C	Crack-growth constant
COD	Crack-opening displacement (m)
c	One-half of surface length of surface crack (m)
f(b/a)	Geometric function in stress intensity solution
K_{EC}	Stress intensity for an edge crack ($N/m^{3/2}$)
K_{eff}	Effective stress intensity range ($N/m^{3/2}$)
K_{Ic}	Fracture toughness value ($N/m^{3/2}$)
K_{RES}	Stress intensity due to residual stresses ($N/m^{3/2}$)
K_S	Stress intensity due to stress S ($N/m^{3/2}$)
K_{SC}	Stress intensity for a surface crack ($N/m^{3/2}$)
n	Crack-growth exponent
P	Applied load or concentrated force (N)
Q	Surface crack shape factor
S	Externally applied stress (N/m^2)
δ	Depth-of-shot-peening parameter (m)

ΔK_{eff}	Range of stress intensity ($N/m^{3/2}$)
σ_C	Compressive residual stress (N/m^2)
σ_T	Tensile residual stress (N/m^2)
$\frac{da}{dN}$	Crack growth per cycle (m)

Residual Stress Model

General

Most machining operations and surface treatments leave residual stresses in the material. The distribution and depth of these residual stresses depend on the particular process. The D6AC material used in this investigation probably contained residual stresses caused by rolling, heat-treating, and shot-peening processes. These residual stresses were not measured for this study. Rather, their distribution was estimated from earlier measurements of residual stresses caused by the machining and surface treatments [1].

When a crack is growing through a shot-peened surface, the stress intensity at the crack front is influenced by the residual stresses. The effect of these stresses is to cause the crack to remain closed until the externally applied stress can overcome the action of the residual stresses. The effective stress intensity of the crack tip is obtained by superimposing the solution for the stress intensity due to external loading and the solution for the stress intensity due to the residual stresses. The crack will open when the effective stress intensity is positive.

Methods exist for the analysis of the stress intensity at the tip of a crack due to these residual stresses. The distribution of stresses and the stress intensity calculation are described in the next two sections.

The Residual Stress Distribution

The residual stress distribution caused by shot-peening is compressive near the surface and tensile to some depth below the surface. To simplify the stress intensity calculation a piecewise linear residual stress distribution was assumed. The shape of this distribution is given to Figure 1.

Three parameters define the assumed residual stress distribution. The depth of the constant compressive stress is δ, the remaining stress distribution defined in multiples of δ. The compressive stress is σ_C, and the peak value of the residual tensile stress is σ_T. When a flaw exists in a shot-peened surface, a surface crack originating at the flaw must grow through this residual stress field. The model derived here is designed to calculate the influence of the residual stress field on the fracture and cyclic crack-growth behavior of such a surface crack.

Determination of Stress Intensity

For a linear distribution of stress on the surface of an edge crack, a closed-form solution for the stress intensity was obtained by Benthem and Koiter [2]. This solution is shown in part (a) of Figure 2. It was used for the analysis of stress intensities for crack lengths shallower than δ.

To obtain a solution for cracks deeper than δ, the piecewise linear distribution was divided into a series of concentrated force pairs. A solution for a single force pair is given in Reference [3], and shown in part (b) of Figure 2. The residual stress intensity K_{RES} was obtained by the summation,

$$K_{RES} = \sum K_i \tag{1}$$

where K_i is given in Figure 2, and the P_i are the equivalent concentrated forces substituted for the residual stress distribution.

The analytical approximation shown in Figure 2 for the function f(b/a) was obtained by fitting a curve to the numerical results presented in [3].

The Surface Flaw

The solutions described for the stress intensity due to residual stresses apply to an edge crack or to a surface crack of $a/2c = 0$. To apply the solutions to a surface crack of semicircular shape, the stress intensity for the edge crack K_{EC} is divided by the square root of the surface flaw shape factor Q.

$$K_{SC} = K_{EC}/\sqrt{Q} \tag{2}$$

Fracture Strength

The fracture strength of a cracked component is determined by the effective crack front stress intensity and the fracture toughness of the material. The effective stress intensity is the sum of the residual stress intensity K_{RES}, and the stress intensity from the applied stress S,

$$K = K_{RES} + K_S \tag{3}$$

At fracture the effective stress intensity is equal to the material's fracture toughness, so that

$$K_{RES} + K_S = K_{Ic} \tag{4}$$

The residual stress intensity K_{RES} can be obtained from the calculation described by Equation (1). The stress intensity caused by the applied loading S is given by

$$K_S = 1.12\, S\sqrt{\frac{\pi a}{Q}} \tag{5}$$

Equations (1), (4), and (5) can be combined to obtain the fracture strength,

$$S = (K_{Ic} - K_{RES}) \Big/ 1.12\sqrt{\frac{\pi a}{Q}} \tag{6}$$

Cyclic Crack Growth

The rate of cyclic crack growth is assumed to be a function of the effective stress intensity of the form

$$\frac{da}{dN} = C\,(\Delta K_{eff})^n \tag{7}$$

For zero-to-tension loading, and a residual stress intensity K_{RES}, Equation (5) becomes

$$\frac{da}{dN} = C\,(K_S + K_{RES})^n \tag{8}$$

for

$$(K_S + K_{RES}) \geq 0$$

Experiments

General

As part of the F-111 Recovery Program, fracture strength tests and cyclic crack-growth tests were conducted on specimens cut from several plates of "low-toughness" D6AC steel. The general mechanical properties of this material have been summarized in [4]. That report presents results of studies from several laboratories including Langley Research Center.

The tests reported herein were carried out on the same stock of material as the tests reported in [4]. The plates from which specimens were cut had been shot-peened and cadmium-plated. As part of the present study, a small number of specimens were loaded to a permanent compressive strain of 0.1 percent to eradicate the residual stresses caused by shot-peening. These precompressed specimens were then used to generate a new set of fracture strength and crack-growth data for comparison with the data from the shot-peened material.

Specimens

Hour-glass shaped specimens (Fig. 3) were cut from the plate stock. The center line was parallel to the rolling direction. Semicircular notches were electromachined into the test section to start the fatigue cracks.

Fracture strength test specimens were precracked to the desired crack depth at (275 MN/m^2) stress range by applying zero-to-tension cyclic loads.

Instrumentation

Crack depth was monitored by the compliance technique using the NASA COD – gage (Fig. 4). The gage length of this gage is 1.2 mm. The electrical signals representing load and crack-opening displacement (COD) were displayed on an X-Y oscilloscope; compliances – and hence crack lengths – were computed from photographic records of the display using an equation

$$\frac{d}{dB}(COD) = A + Ba$$

The constants A and B had previously been determined for the gages used.

Loading

The specimens were loaded uniaxially in a 1.8-MN-capacity servo-hydraulic testing machine. The test frequency for cyclic crack-growth tests was 3 Hz. The load rate for fracture tests was 15 KN/sec.

Environment

Cyclic crack-growth tests were conducted in laboratory air at 283 K and 70 percent RH. Fracture strength tests were conducted in a dry gaseous nitrogen atmosphere at 233 K. (-40°)

Results and Discussion

Fracture Strength

Figure 5 shows the fracture strengths for eight shot-peened specimens tested under cryogenic conditions. The solid line is a line of constant stress intensity fitted to the fracture strength data for the four longest crack lengths. The data for short crack lengths deviate markedly from the constant stress intensity line.

Four additional fracture specimens were tested. These specimens were precompressed to a permanent residual strain of 0.1 percent to remove the residual stresses caused by the shot-peening process. The fracture strengths for these specimens are shown in Figure 6. The solid line in that figure is the same as the constant stress intensity line shown in Figure 5. The fracture strengths obtained for the shorter crack lengths in precompressed specimens do not deviate significantly from the line of constant stress intensity. This leads to the conclusion that the apparent higher toughness for short crack lengths in the shot-peened material (Fig. 5) is caused by residual stresses from the shot-peening.

To test this conclusion, fracture strength calculations were made with the residual stress model. Model parameters were selected to simulate the residual stress distribution assumed to exist in the shot-peened material. The parameters were $\delta = 0.5$ mm, $\sigma_C = 315$ MN/m^2, $\sigma_T = 240$ MN/m^2, and $K_{Ic} = 48$ MN/m$^{3/2}$. Figure 7 shows the predicted fracture strength as a function of crack length for a plate containing a semicircular surface flaw and having a residual stress distribution shown in Figure 1. The dotted line is a line of constant stress intensity based only on external loading ($K_S = 48$ MN/m^2). For short crack lengths, the model predicts that fracture strengths are higher than predicted

by considering the external loading only. This result is consistent with the test results from the shot-peened specimens (Fig. 5).

Cyclic Crack Growth

Figure 8 shows the crack-growth rate for zero-to-tension loading as a function of the stress intensity range for the shot-peened material. The data from tests at three stress levels (275 MN/m^2, 414 MN/m^2, and 690 MN/m^2) fall along distinctly separate curves. The dotted line represents cyclic crack-growth data obtained from compact tension specimens in investigation [4]. In that investigation cracks were grown from the edge of the plate and, therefore, were less affected by the shot-peening residual stresses.

Figure 9 shows cyclic crack-growth data from three specimens after a pre-compression cycle. The stress levels in this investigation were identical to those for the data of Figure 8. The dotted line in Figure 9 is the same reference line as shown in Figure 8.

The data from the precompressed specimens agree with the data from the compact tension tests, and can be described by the Paris' Law, where

$$\frac{da}{dN} = C\,(\Delta K)^n \tag{9}$$

and

$$C = 1.87 \times 10^{-12} \qquad n = 2.72$$

To show that the stress-level effect shown in Figure 8 for shot-peened specimens is caused by the residual stresses, the effect of the residual stresses on the cyclic crack-growth rate was calculated with Equation (8). The model parameters were the same as those used for the fracture strength calculations.

Figure 10 shows the calculated cyclic crack-growth rates as a function of the stress intensity range K_S, the stress intensity due to the external loading.

The three curves labeled with stress levels represent the computed crack-growth behavior for those three stress levels used in the experiment. The curve labeled "No Residual Stress" represents the basic Equation (9).

The model calculations showed that the residual stress intensity was negative for crack lengths smaller than 1.3 mm, and was positive for crack lengths larger than 1.3 mm.

For crack lengths shorter than 1.3 mm the crack-growth rates were lower than predicted by Paris' Law; for crack lengths larger than 1.3 mm, crack-growth rates were faster than predicted by Paris' Law.

The results in Figure 10 show that for lower values of applied stress the crack-growth rate is higher for the same stress intensity range. This result is qualitatively the same as that obtained experimentally from the shot-peened material.

Conclusion

1. The fracture strength and cyclic crack-growth properties of D6AC steel were affected by the residual stresses left by the shot-peening.

2. Compression residual stress near the surface caused shallow cracks to grow more slowly than observed for cases without residual stress. Tension residual stresses below the shot-peened layer caused deeper cracks to grow more rapidly than observed for cases without residual stress.

3. Compression residual stresses near the surface gave shallow cracks an apparent fracture toughness higher than the fracture toughness of the stress-free material. Tension residual stresses below the shot-peened layer gave deeper cracks an apparent fracture toughness lower than the fracture toughness of the stress-free material.

4. A simple model based on the contribution of the residual stress to the effective stress intensity explains the trends in both fracture strength and cyclic crack growth.

References

[1] Koster, W. B., Field, M., Fritz, L. J., Gatto, L. R., and Kahles, J. F., "Surface Integrity of Machining Structural Components," Technical Report AFML-TR-70-11, March 1970.

[2] Benthem, J. P., and Koiter, W. T., Asymptotic Approximations to Crack Problems, Mechanics of Fracture, Noordhoff International Publishing, Leyden, 1972.

[3] Hartranft, R. J., and Sih, G. C., "Alternating Method Applied to Edge and Surface Crack Problems," Lehigh University, Technical Report IFSM-72-13, April 1972.

[4] Fedderson, C. E., Moon, D. P., and Hyler, W. S., "Crack Behavior in D6 AC Steel," Metals and Ceramics Information Center, MCIC-72-04, January 1972.

TABLE 1. CHEMICAL COMPOSITION AND MECHANICAL PROPERTIES OF D6AC STEEL

Chemical Composition			
Element	Percent	Mechanical Properties	
C	0.48	Yield strength	1450 MN/m^2
Mn	0.83	Ultimate strength	1600 MN/m^2
P	0.01	Elongation	14%
S	0.005		
Si	0.28		
Ni	0.58		
Cr	1.06		
Mo	1.01		
V	0.1		
Cu	0.15		

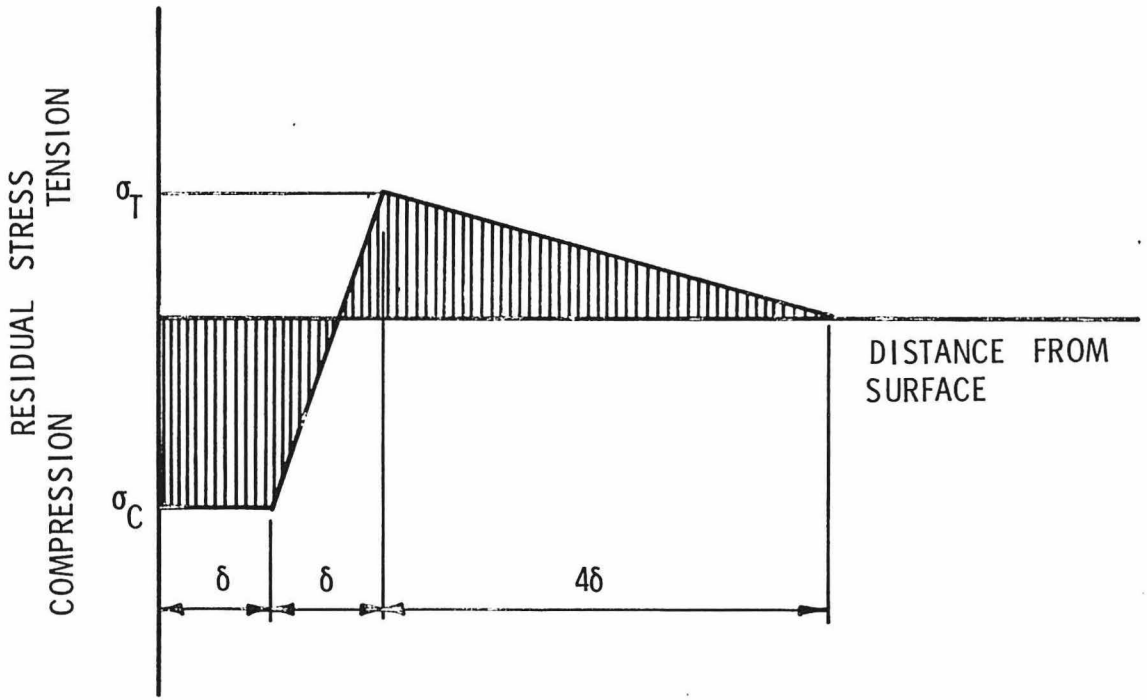

Figure 1. Estimated residual stress distribution

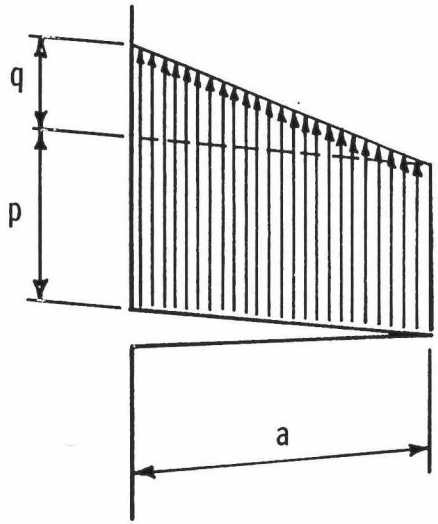

$$K_{EC} = (1.122\ p + 0.439\ q)\sqrt{\pi a}$$

a) Distributed Stress

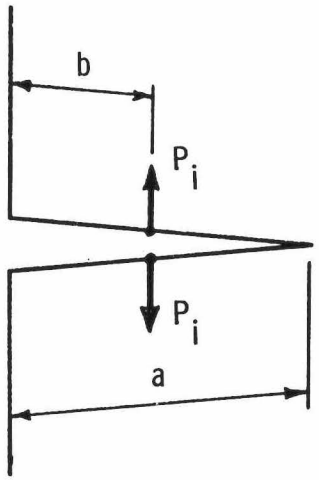

$$K_i = \frac{2\ P_i \left[1 + f(b/a) \right]}{\sqrt{\pi}\ \sqrt{a^2 - b^2}} \sqrt{\pi a}$$

$$f(b/a) \approx 0.35\ (1 - b/a) - 0.055\ (1 - b/a)^7$$

b) Concentrated Force

Figure 2. Stress intensity solutions for edge cracks

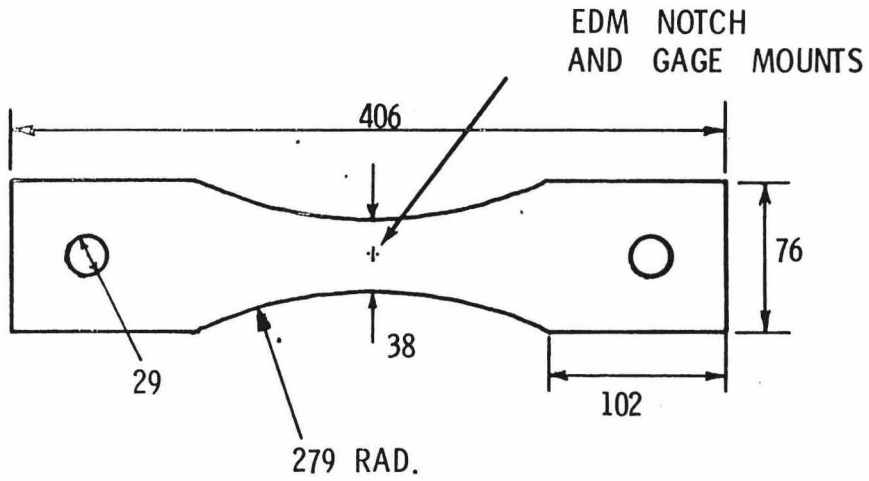

Figure 3. Specimen configuration (Dimensions in mm)

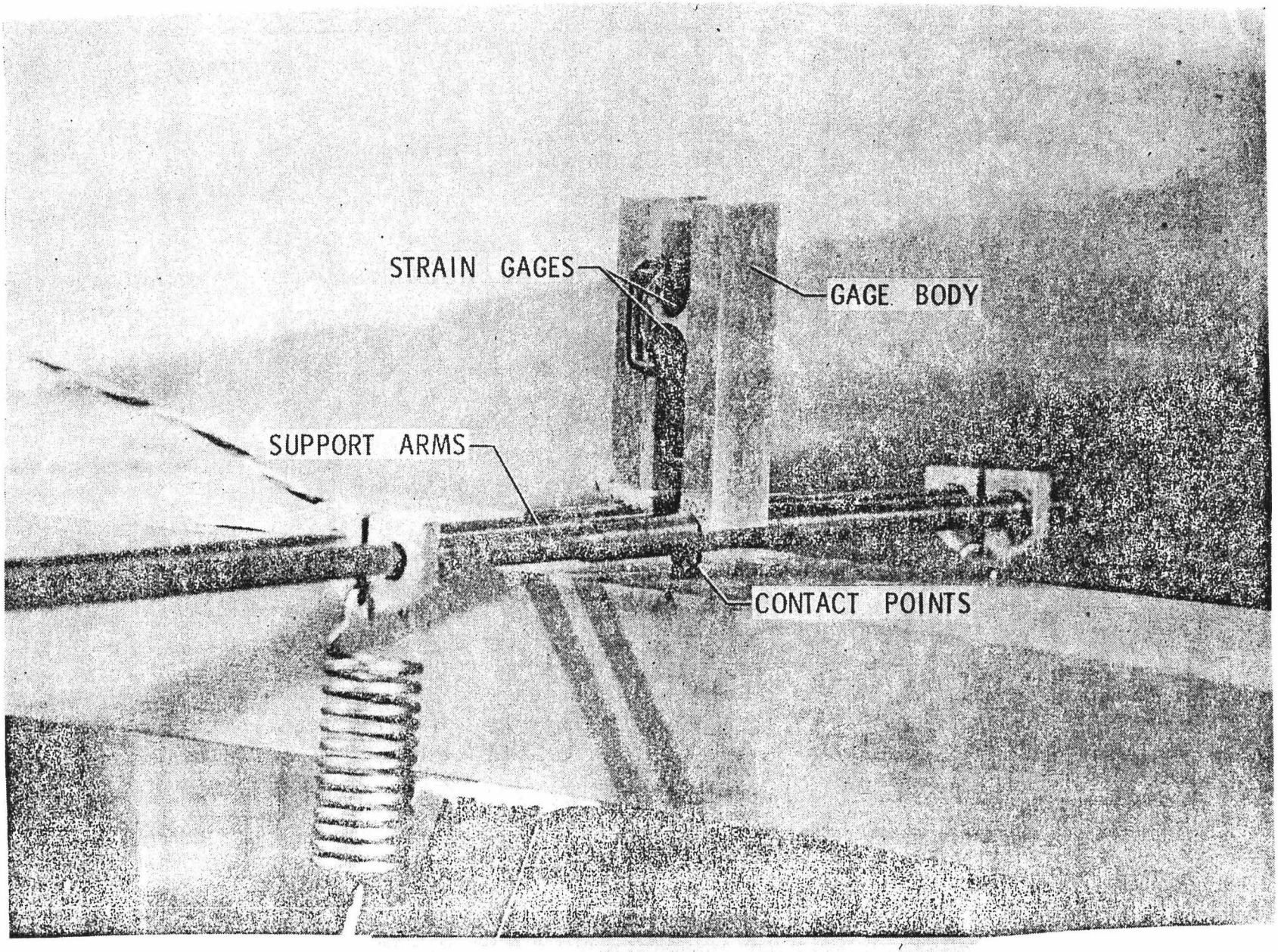

Figure 4. NASA COD - gage. Gage length 1.2 mm.

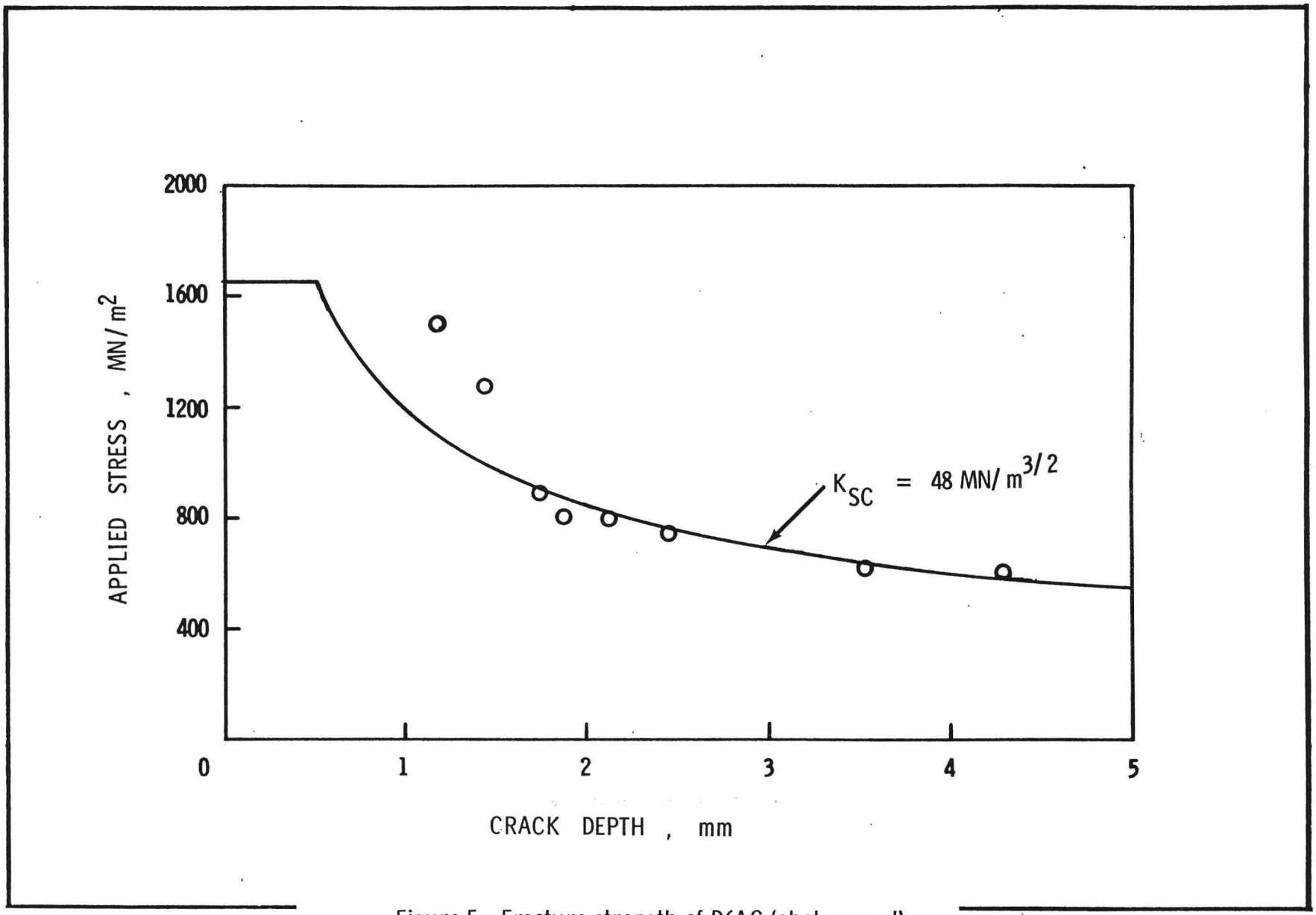

Figure 5. Fracture strength of D6AC (shot-peened)

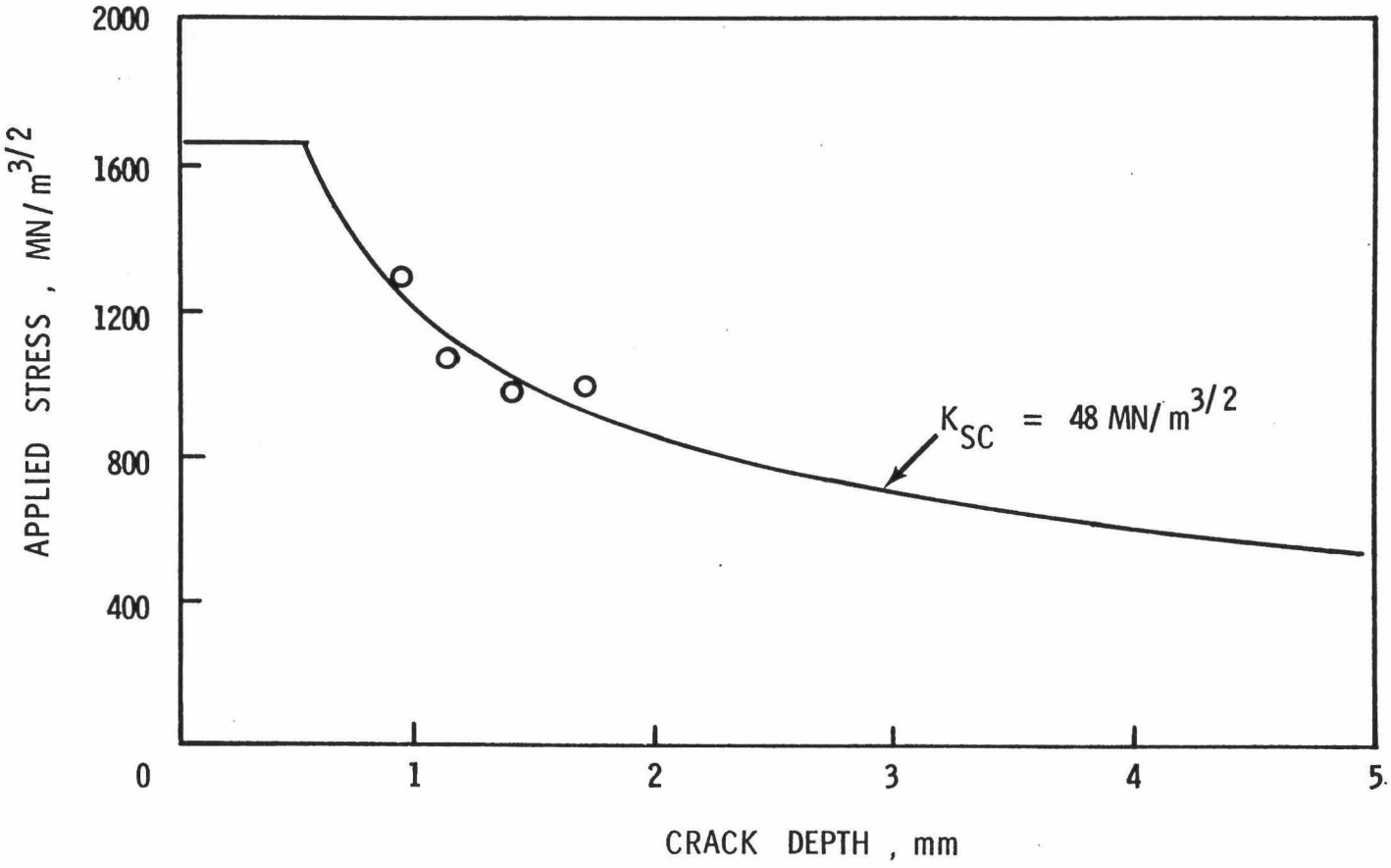

Figure 6. Fracture strength of D6AC (shot-peened and precompressed)

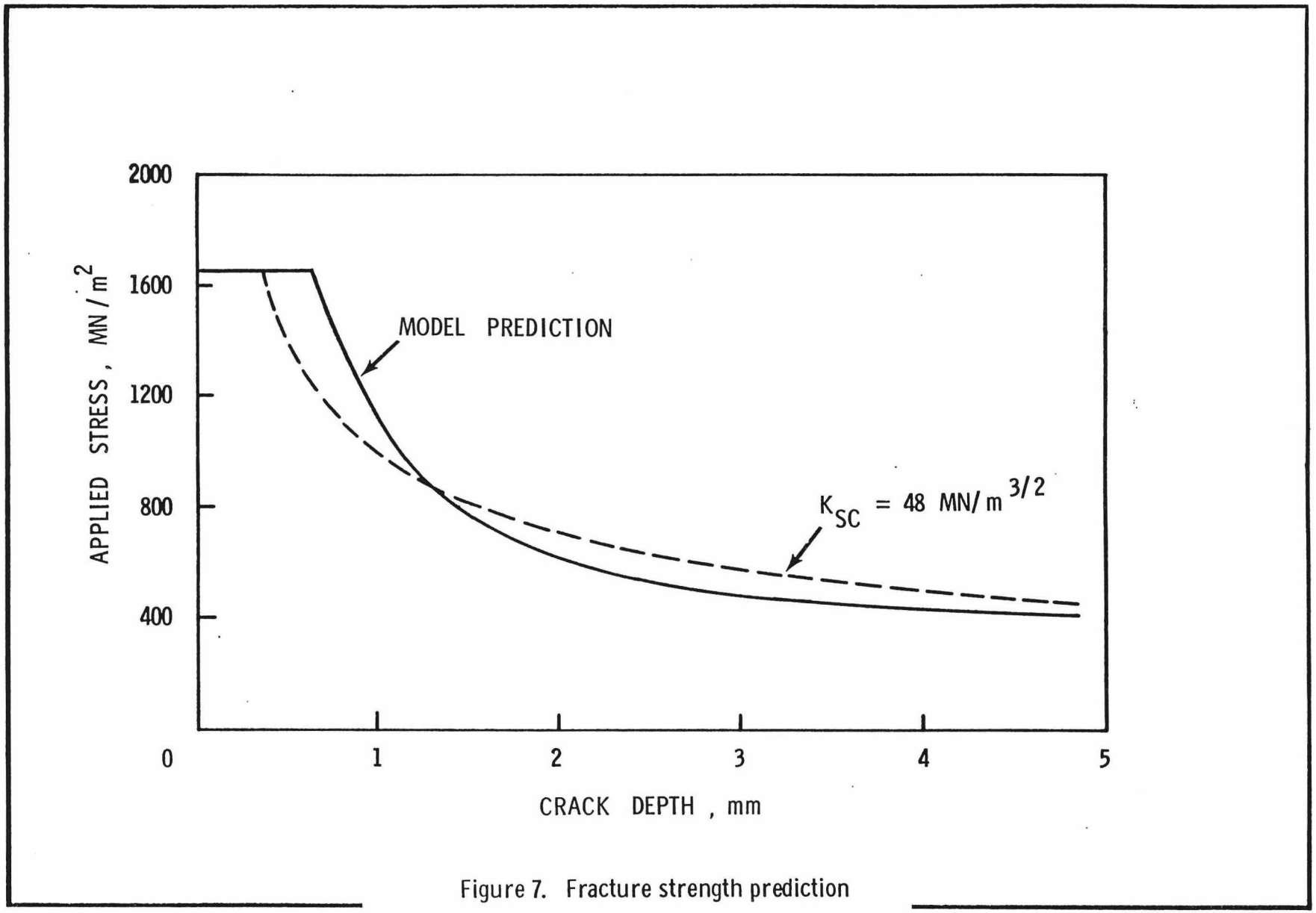

Figure 7. Fracture strength prediction

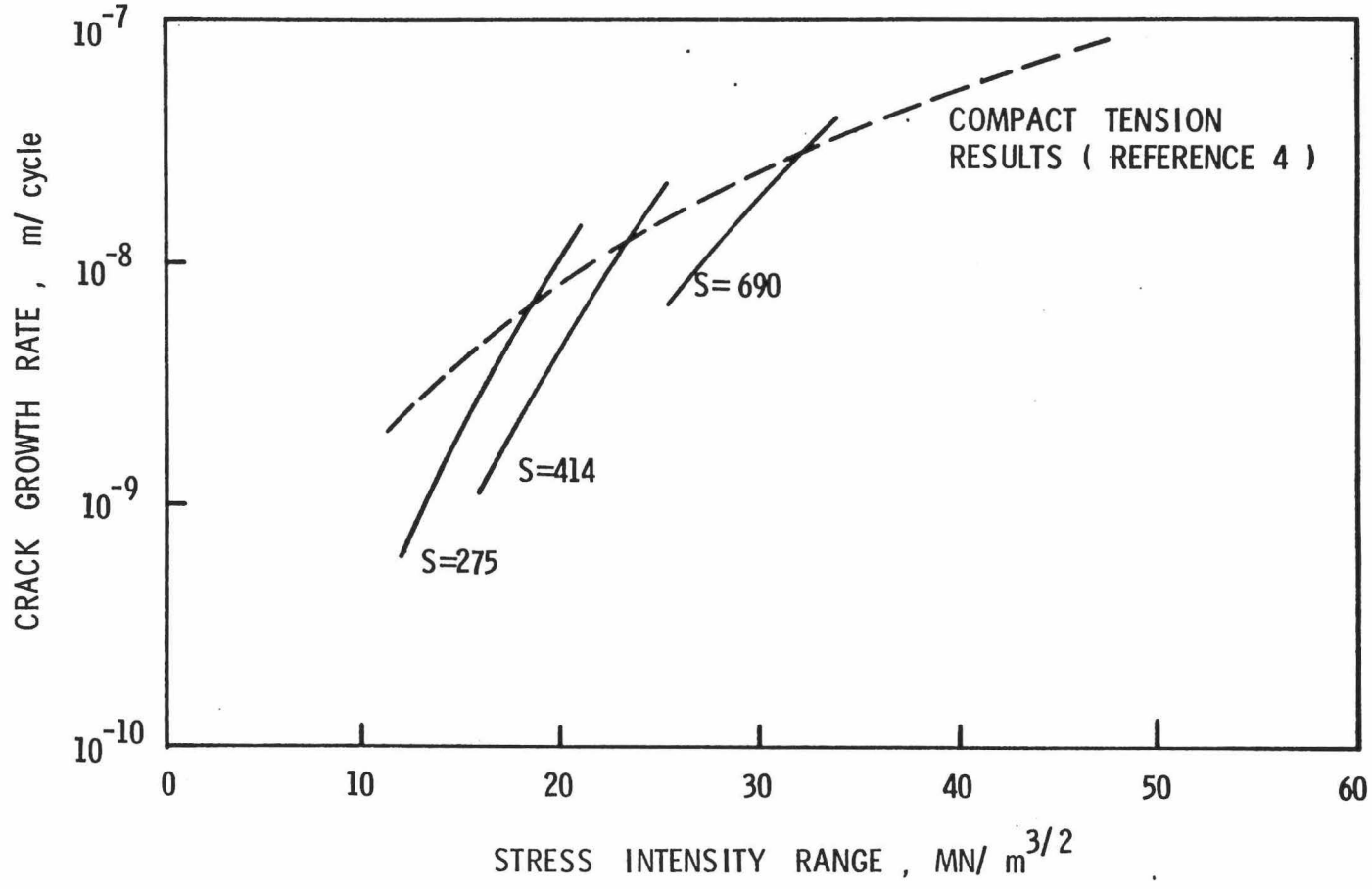

Figure 8. Crack-growth rates for D6AC (shot-peened)

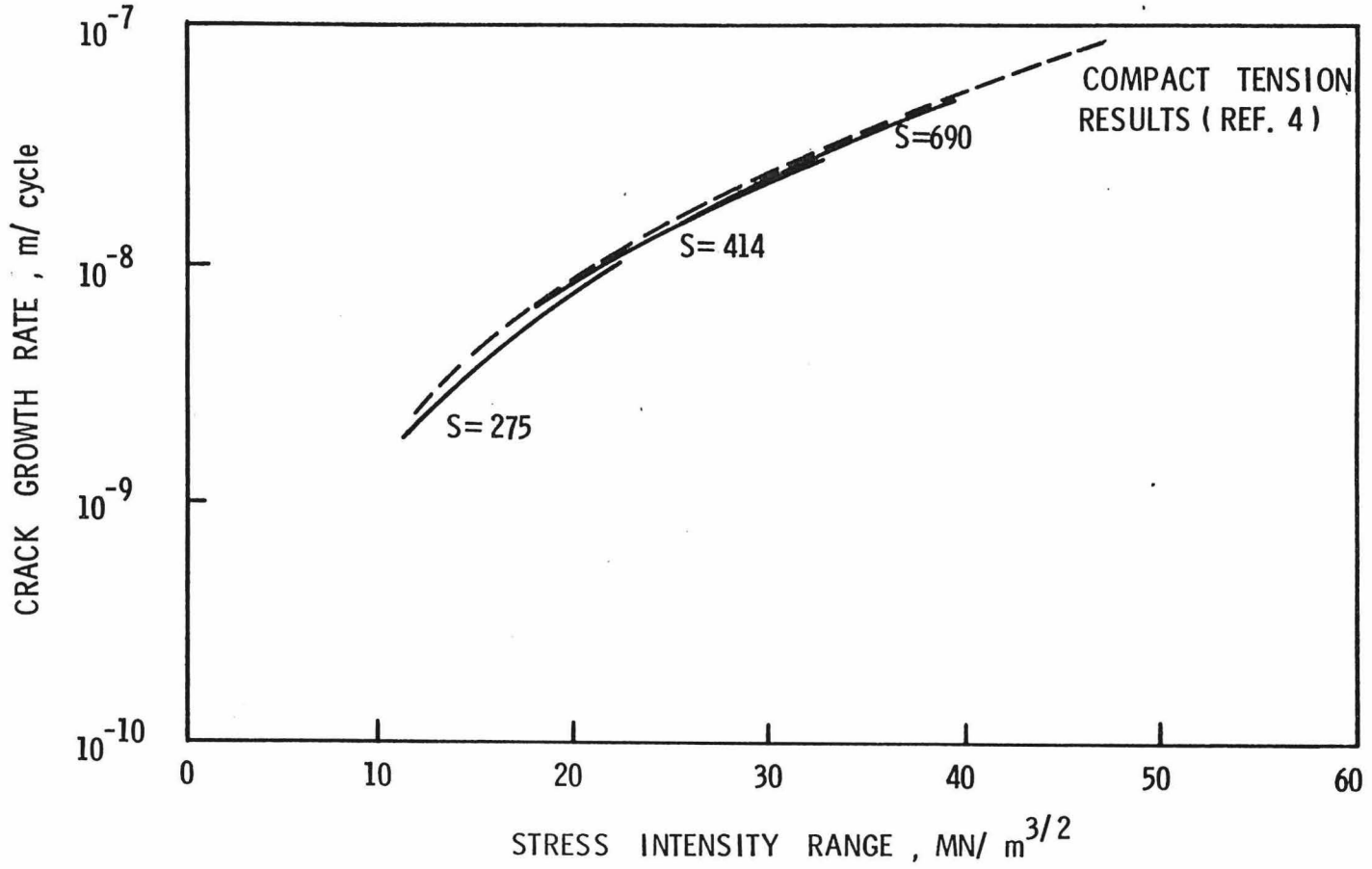

Figure 9. Crack-growth rates for D6AC (shot-peened and precompressed)

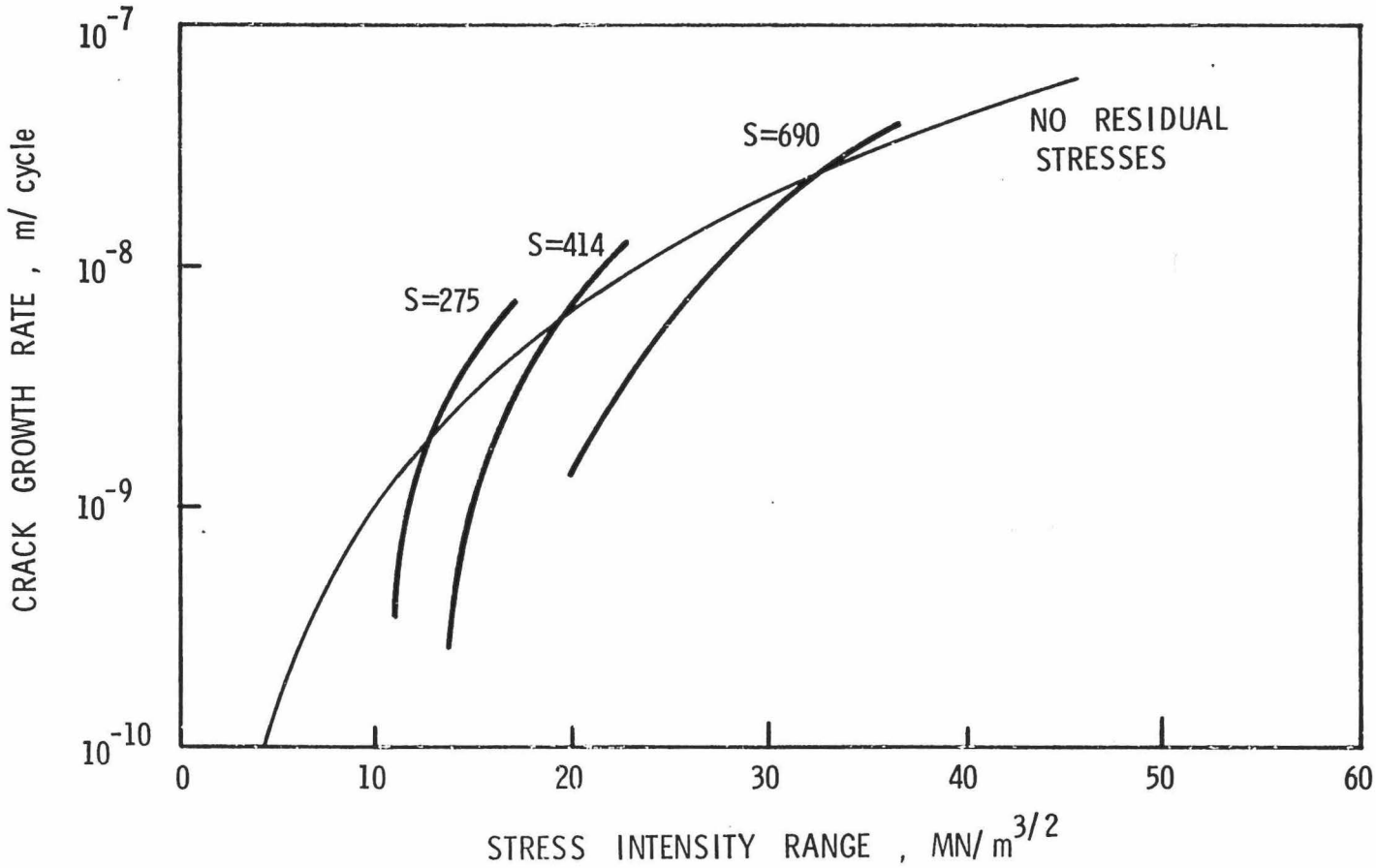

Figure 10. Crack-growth rate prediction